Heat Transfer in Magma in situ

Abstract. *Heat transfer rates in a basaltic magma were measured under typical magma chamber conditions and a numerical model of the experiment was used to estimate magma viscosity. The results are of value for assessing methods of thermal energy extraction from magma bodies in the upper crust as well as for modeling the evolutionary track of these systems.*

Knowledge of convection in magmatic systems is crucial to assessing the feasibility of direct energy extraction from shallow magma bodies in the earth's crust (*1*). Furthermore, heat transfer in magmas strongly influences the flow of heat to the earth's surface, affecting processes such as mineralization and thermal metamorphism. While convective heat transfer rates have been measured in degassed basaltic magmas at atmospheric pressure and near-liquidus temperatures (*2*), similar heat transfer measurements have not, to our knowledge, been made for a magma with volatiles at representative in situ temperatures and pressures. However, there is reason to believe that pressure and, particularly, volatile content influence convective heat transfer by lowering magma viscosity (*3–5*). We report a novel laboratory investigation of magma convection in a low-silica basalt under conditions of temperature, pressure, and water content corresponding to those in a magma chamber at a depth of 7.5 km. In contrast to previous heat transfer measurements in magma, the controlled conditions of this experiment allow detailed numerical modeling from which viscosity in a naturally convecting magma can be inferred. This combination of measurement and modeling is necessary for scaling convection to crustal magma bodies.

In situ temperature and pressure conditions were simulated at Sandia National Laboratories in a large-volume, high-pressure, and high-temperature autoclave. A platinum crucible with a sample volume of about 0.5 liter was fabricated for these convection experiments (Fig. 1). The inner boundary of the crucible was designed to accept an axial heater. This configuration produced a constant heat flux along the inner boundary while the outer boundary was held at a constant temperature by the autoclave control system. Upper and lower boundaries were insulated with eight alternating layers of ceramic fiber blanket and molybdenum radiation reflectors. Temperatures along the inner and outer boundaries were measured with Pt/Pt-Rh thermocouples welded to the crucible in six places. For the sample we used a local New Mexico alkali basalt (Cuberio basalt), containing 46 percent silica by weight (*6*), that was used in previous heat transfer measurements at atmospheric pressure (*2*).

To interpret the temperature data, numerical modeling was carried out with a general-purpose, two-dimensional computer program. This finite-element code solves the axisymmetric, free convection problem using the Boussinesq form of the Navier-Stokes equations (*7*). Constant thermal properties appropriate for a basaltic magma at high temperature were used in the calculations (*8*). The model was "started up" in the same fashion as the actual apparatus. At zero time the model was isothermal, having a temperature equal to the temperature of the outer external wall of the platinum container. At this time a constant heat flux was applied to the inner boundary. As the molten region began to heat, convective circulations developed, and after 2500 to 3000 seconds a steady-state thermal distribution was obtained. The numerical calculations show that steady-state conduction produces a nearly symmetrical temperature distribution along the inner boundary, with a maximum near the midpoint. On the other hand, thermally driven circulations in the molten basalt create a skewed temperature distribution along the boundary, with a maximum shifted upward away from the midpoint. The boundary temperature distribution (Fig. 2) is illustrative of skewing caused by convection. Further, the mean temperature of the inner boundary is as much as 38°C lower in the presence of convection. In the interior, isotherms are more or less vertical in the conductive runs, but with convective circulation they are distorted in the direction of fluid motion (up along the heated inner wall and down along the cooler outer wall). Besides affecting the distribution of isotherms, convection provides more efficient heat transfer across the test section. The laboratory results also exhibit these features, which are characteristic of convection. In fact, inner boundary temperatures could be closely matched only when convection was included in the calculated model.

Figure 3 shows the results of test runs at nearly constant power (68 W). The effect of convection is quantified by calculating a form of the Nusselt number, the ratio of the total heat transfer rate to the rate of heat transfer by conduction only (*9*). The data clearly show an increase in heat transfer rate with increasing mean temperature. This same trend with mean temperature was also observed in preliminary experimental runs with dry Cuberio basalt (*10*). However, the present data result in heat transfer coefficients that are approximately 30 percent higher than the dry values ob-

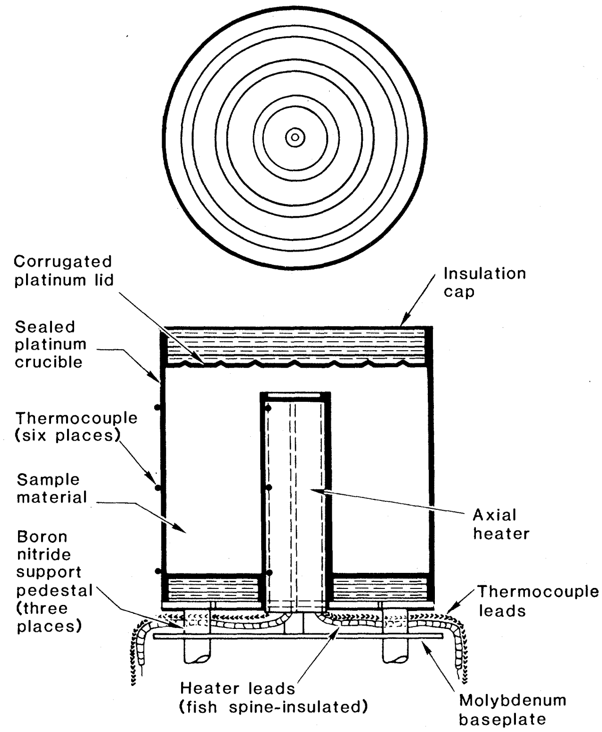

Fig. 1. Top and cross-sectional views of the platinum crucible test section. Zirconium-stabilized platinum sheet stock, 0.51 mm thick, was used for all boundaries. The lid of the crucible was corrugated in the form of concentric circles to allow for significant changes in internal volume during heating. The internal crucible is 0.090 m in diameter by 0.081 m in height. The axial heater finger is 0.019 m in diameter and extends 0.075 m into the sample material. During an experiment, the central heater provides constant heat flux on the inner wall while the outer wall is maintained at a constant temperature in an argon environment. Thermocouples are mounted at six locations on the inner and outer walls of the apparatus.

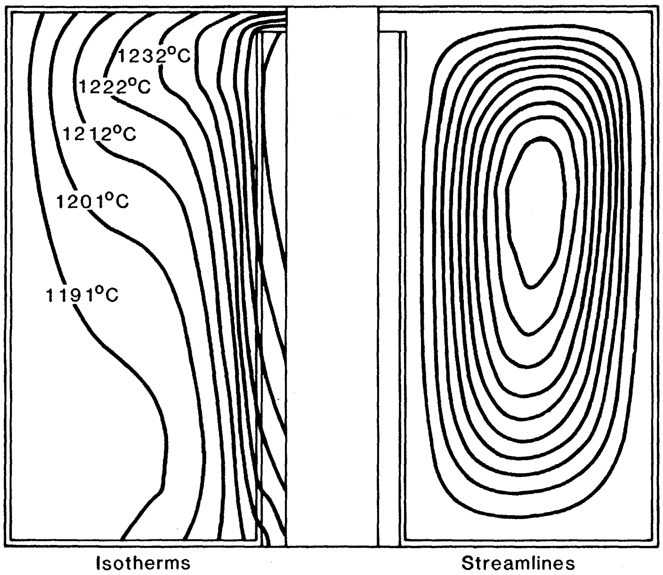

Fig. 2. Schematic showing isotherms and streamlines predicted by the numerical model for a total heat flux of 73 W on the inner wall and a constant temperature of 1180°C on the outer. The relatively low value of the dynamic viscosity (20 P) allows convection to be vigorous enough to strongly distort the isotherms, introducing asymmetry into the inner wall temperature distribution.

tained at the same mean temperature. We conclude that the addition of water significantly increases convective heat transfer rates.

The influence of viscosity on heat transfer was numerically evaluated for several different constant viscosity values (10 to 200 poise). (The use of constant viscosity rather than a more complicated, temperature-dependent rheology was deemed adequate for bounding values of the Nusselt number in the experiment.) Each calculation results in a single Nusselt value, giving rise to the horizontal lines shown in Fig. 3. As expected, lower viscosity runs correspond to higher rates of heat transfer. The numerical calculations were also used to evaluate the effect of temperature-dependent thermal conductivity. Over the range of temperatures considered, the data of Murase and McBirney (*11*) show a ±17 percent variation from the constant value of thermal conductivity used. The effects of this maximum variation, calculated for the 20- and 100-P cases, are illustrated by the shaded zones in Fig. 3. A ±17 percent variation in thermal conductivity results in a ±4 percent variation in heat transfer at the lower viscosity and approximately a ±2 percent variation at the higher viscosity. Thus a large variation in thermal conductivity with mean temperature cannot explain the data obtained.

For a water content of 2.7 percent by weight, we find that the experimental data are consistent with viscosities between 200 and 20 P over a mean temperature from 1010° to 1230°C. These results compare favorably with those of Fujii and Kushiro (*3*) and Kushiro *et al.* (*4*), who obtained slightly higher viscosities for a dry Kilauea olivine tholeiite (50 percent silica by weight) at higher pressure. For a pressure of 500 MPa they found viscosities of 63 P at 1270°C and 33 P at 1400°C. At even higher pressures (1500 MPa) they found very little change in the viscosity of dry basalt for comparable temperatures.

Our values are also somewhat lower than viscosities measured by Murase and McBirney (*11*) for dry basalts at atmospheric pressure. At temperatures near 1200°C they obtained viscosities of 630 P for Columbia River basalt (51 percent silica by weight) and 125 P for Galápagos olivine basalt (46 percent silica). The latter silica content is comparable to that of the Cuberio basalt used here. While the viscosities inferred from the present experiment are lower than the above values, the actual variation between wet and dry measurements is not nearly as dramatic as the variation found by Shaw (*5*) for obsidian having a silica content of 77 percent by weight. Since water decreases magma viscosity by reducing the polymerization of silica in the melt, the effect of water on a more weakly polymerized alkali basalt should be less (*5*).

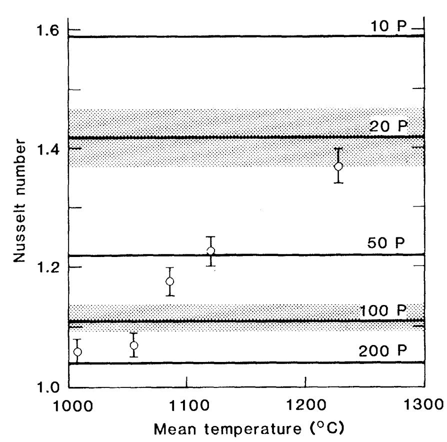

Fig. 3. Dependence of the Nusselt number on the mean temperature of the magma. The five data points presented correspond to experimental runs made with the same value of heat flux applied to the inner boundary but with different prescribed outer boundary temperatures. Error bars at each data point reflect a ±2°C uncertainty in the measurement of temperature difference. Horizontal lines represent numerical calculations of the Nusselt number for the experiment using a constant viscosity model.

We conclude that convective heat transfer is much more effective in magmas in situ than might be expected from measurements obtained with degassed magmas at atmospheric pressure. Further, our ability to successfully model the dynamics of the small-scale convecting system by using accepted values of magma properties provides a basis for numerically extrapolating the heat transfer behavior of magma to large crustal magma bodies. The inferred viscosities are significant for thermal history models of magmatic regions since the ability of volcanic plumbing to remain in the molten state depends on the efficiency of circulations carrying heat from the hotter, resupplied regions to the more remote parts of the system. Conduits and dikes are extreme examples of structures that depend on the vigor of convection to offset heat lost to the host rock if the structure is to remain molten in the absence of a forced flow of magma through the system. For vertical conduits, natural circulations might allow the structure to behave as a heat pipe (*12*), an idea supported by the relatively low viscosities reported here.

J. C. Dunn
C. R. Carrigan
R. P. Wemple
Sandia National Laboratories, Albuquerque, New Mexico 87185

References and Notes

1. H. C. Hardee, *J. Volcanol. Geotherm. Res.* **10**, 175 (1981).
2. ——— and J. C. Dunn, *ibid.*, p. 195; H. C. Hardee, *J. Geophys. Res.* **84**, 7485 (1979); *Science* **222**, 47 (1983).
3. T. Fujii and I. Kushiro, *Carnegie Inst. Washington Yearb.* **76**, 419 (1977).
4. I. Kushiro, H. S. Yoder, B. O. Mysen, *J. Geophys. Res.* **81**, 6351 (1976).
5. H. R. Shaw, *ibid.* **68**, 6337 (1963); *Am. J. Sci.* **263**, 120 (1965); *ibid.* **272**, 870 (1972); in *Geochemical Transport and Kinetics*, A. W. Hofmann *et al.*, Eds. (Carnegie Institution of Washington, Washington, D.C., 1974), pp. 139–170.
6. After machining the test material to the precise internal contour of the crucible, we dehydrated the sample and loaded it into the crucible. The entire assembly was evacuated and then pressurized in deionized water at 3.2 MPa, driving the water into the natural pore space of the sample. The final water content after sealing was 2.7 percent by weight. This corresponded to approximately 65 percent of the water required for saturation at the liquidus.
7. D. K. Gartling, *Comp. Methods Appl. Mech. Eng.* **12**, 365 (1977). The apparatus was modeled on a grid of 169 subparametric rectangular elements that contained the molten basaltic region,

the platinum container walls, and the aluminum oxide core surrounding the central heater.
8. Constant thermal properties used in the numerical modeling are as follows: density, 2630 kg/m^3; specific heat, 1255 J/kg-K; thermal conductivity, 1.255 W/m-K; and coefficient of thermal expansion, 4×10^{-5} K^{-1}.
9. Here Nusselt number is the experimental heat transfer coefficient divided by the heat transfer coefficient obtained from the numerical model for pure conduction. The experimental coefficient is a function of mean temperature and is given by

$$h = \frac{Q}{A(T_i - T_o)}$$

where Q is heater power, A is area of the inner wall of the crucible, and T_i and T_o are average inner and outer wall temperatures, respectively.
10. J. C. Dunn, C. R. Carrigan, R. P. Wemple, *Eos* **62**, 1055 (1981).
11. T. Murase and A. R. McBirney, *Geol. Soc. Am. Bull.* **84**, 3563 (1973).
12. C. R. Carrigan, *J. Volcanol. Geotherm. Res.* **16**, 279 (1983).
13. We thank D. K. Gartling for help with the numerical modeling, H. R. Westrich for chemical analysis of the sample material, and J. A. Rejent for technical support at the magma simulation facility. R. J. Hunter skillfully typed the manuscript.

21 July 1983; accepted 13 October 1983

Mesozoic Mammals from Arizona: New Evidence on Mammalian Evolution

Abstract. *Knowledge of early mammalian evolution has been based on Old World Late Triassic–Early Jurassic faunas. The discovery of mammalian fossils of approximately equivalent age in the Kayenta Formation of northeastern Arizona gives evidence of greater diversity than known previously. A new taxon documents the development of an angular region of the jaw as a neomorphic process, and represents an intermediate stage in the origin of mammalian jaw musculature.*

Knowledge of the emergence and early evolution of mammals has been based upon faunas of Late Triassic–Early Jurassic age from localities throughout the Old World (*1, 2*). Best known and most common are representatives of the Morganucodontidae, a family of triconodonts allied to later groups of Mesozoic mammals (*3*); morganucodontids are known from England and Wales, continental Europe, China, and southern Africa. Another family, the Kuehneotheriidae, is known solely from isolated teeth and fragmentary maxillae and mandibles found in fissure deposits in Wales; the molars nonetheless give evidence that *Kuehneotherium* was of the stock that gave rise to later therian mammals (*4*). Most other mammalian fossils of comparable age are too incomplete to establish their affinities with confidence (*5*). Until recently, we interpreted the major event of early mammalian evolution as a dichotomous branching of morganucodontids (nontherians) and kuehneotheriids (therians) during the latter half of the Triassic (*3*). In this report of the first discovery of a morganucodontid fauna in the New World, we also describe a previously unknown mammal, and present evidence that modifies previous interpretations of early mammalian anatomy and evolution.

The fossil mammals were discovered in the silty facies of the Kayenta Formation exposed along the Adeii Eechii Cliffs about 30 miles south-southeast of Tuba City, Arizona (*6*). The associated vertebrate fauna includes ornithischian and saurischian dinosaurs, crocodilians, tritylodontids, turtles, lizards, amphibians, and pterosaurs (*7*). Two taxa, the small tritylodontid *Oligokyphus* (*8*) and a morganucodontid, are congeneric with forms from European deposits.

The morganucodontid remains are fragmentary; they consist of a crushed skull, postcranial bones, and four isolated teeth. A well-preserved left upper molar (Fig. 1, a and b) shows the configuration of cusps *A–F*, and the presence of a large external and a smaller internal cingulum, all morganucodontid characteristics (*9*). The dimensions of the crown (length, 1.11 mm; width, 0.64 mm) are within the observed ranges of the Welsh morganucodontid *Morganucodon watsoni* and those of the Chinese species (*10*). However, several features of the Kayenta morganucodontid molar are distinctive. Cusp *B* is more robust than cusp *C*. The internal cingulum, which is typically complete in *M. watsoni*, has a hiatus at its midpoint. The large size of the cuspules on the external cingulum is more similar to that of the southern African *Megazostrodon* than to that of the Welsh morganucodontid. These features are probably indicative of a species difference, but for lack of more complete material at present we simply refer the Kayenta morganucodontid to *Morganucodon* sp.

One specimen may provide evidence of haramiyids, an enigmatic group of mammals [possibly ancestral to multituberculates (*11*)] that occurs as rare fossils in Rhaeto-Liassic deposits of Europe. The tooth (Fig. 1c) bears several features characteristic of *Haramiya*: two rows of cusps, joined at one end by a crest, enclose a central sulcus; one row bears three cusps; the largest cusp of the other row is adjacent to the open end of the sulcus, and there are three roots, two of which form a pair below the open end of the sulcus. Unlike *Haramiya*, however, the second row bears only two cusps (rather than four or five), and the tooth is smaller (0.66 mm long) than European specimens (1 to 3 mm) (*2, 12*). Haramiyids are insufficiently known to assess the significance of these differences, but their occurrence with *Morganucodon* strengthens the correlation with Rhaeto-Liassic vertebrate faunas of Europe.

More abundant and better preserved are specimens of a new mammalian taxon:

Class: Mammalia
Order: Triconodonta
Family incertae sedis
Dinnetherium gen. nov.

Etymology: Dinne, the Navajo Indian word for the (Navajo) people; Thērion, Greek, wild beast: the "Navajo's wild beast."
Type species: *Dinnetherium nezorum* sp. nov.
Diagnosis: As for the type and only species.

Dinnetherium nezorum sp. nov.
Etymology: Named for the Nez family of Gold Spring.
Type: MNA V3221, a partial right mandible with $M_{2\text{–}5}$.
Referred material: MCZ 20870–20877.
Diagnosis:

$$I\frac{?}{4}\ C\frac{?}{1}\ PM\frac{2+?}{4}\ M\frac{5}{5}$$

Three primary cusps on molariforms aligned anteroposteriorly as in morganucodontids, but central cusps *A*, *a* are taller as in *Kuehneotherium*. Adjacent molariforms interlock (Fig. 1) by cuspules *e* and *f* (*E* and *F*), forming an embrasure to receive the base of cuspule *d* (*D*) on the next anterior tooth. Cusp *a* occludes between *B* and *A* to produce a nearly horizontal, V-shaped facet that obliterates *B* in stages of advanced wear; cusp *A* produces a nearly vertical facet on *c*. The new species is distinguished from morganucodontids and *Kuehneotherium* by a flange-like ventrolateral extension of the lateral ridge of the dentary, and from triconodontids and amphilestids by the presence of a pseudangular process (*13*).

Dental occlusion and jaw movement, reconstructed from matching wear facets on associated mandibular and maxillary teeth, involved a combination of medial translation and rotation (*14*). Primary cusp *a* of lower molars was the first to make intercuspal contact, and wore be-